Title

Regional variations in MR relaxation of hip joint cartilage in subjects with and without femoralacetabular impingement

Journal

Magnetic Resonance Imaging, 31(7)

ISSN

0730-725X

Authors

Subburaj, Karupppasamy
Valentinitsch, Alexander
Dillon, Alexander B
et al.

Publication Date

2013-09-01

DOI

10.1016/j.mri.2013.01.009

Peer reviewed

Published in final edited form as:
Magn Reson Imaging. 2013 September ; 31(7): 1129–1136. doi:10.1016/j.mri.2013.01.009.

Regional variations in MR relaxation of hip joint cartilage in subjects with and without femoralacetabular impingement☆,,☆☆

Karupppasamy Subburaj[a,*], **Alexander Valentinitsch**[a], **Alexander B. Dillon**[a], **Gabby B. Joseph**[a], **Xiaojuan Li**[a], **Thomas M. Link**[a], **Thomas P. Vail**[b], and **Sharmila Majumdar**[a]

[a]Musculoskeletal Quantitative Imaging Research, Department of Radiology and Biomedical Imaging, University of California, San Francisco, CA 94158, USA

[b]Department of Orthopaedic Surgery at the University of California, San Francisco, CA, USA

Abstract

The objective of this study was to analyze regional variations of magnetic resonance (MR) relaxation times ($T_{1\rho}$ and T_2) in hip joint cartilage of healthy volunteers and subjects with femoral acetabular impingement (FAI). Morphological and quantitative images of the hip joints of 12 healthy volunteers and 9 FAI patients were obtained using a 3 T MR scanner. Both femoral and acetabular cartilage layers in each joint were semi-automatically segmented on sagittal 3D high-resolution spoiled gradient echo (SPGR) images. These segmented regions of interest (ROIs) were automatically divided radially into twelve equal sub-regions (30^0 intervals) based on the fitted center of the femur head. The mean value of $T_{1\rho}/T_2$ was calculated in each subregion after superimposing the divided cartilage contours on the MR relaxation ($T_{1\rho}/T_2$) maps to quantify the relaxation times. $T_{1\rho}$ and T_2 relaxation times of the femoral cartilage were significantly higher in FAI subjects compared to healthy controls (39.9 ± 3.3 msec in FAI vs. 35.4 ± 2.3 msec in controls for $T_{1\rho}$ (P = 0.0020); 33.9 ± 3.1 msec in FAI vs. 31.1 ± 1.7 msec in controls for T_2 (P = 0.0160)). Sub-regional analysis showed significantly different $T_{1\rho}$ and T_2 relaxation times in the anterior-superior region (R9) of the hip joint cartilage between subjects with FAI and healthy subjects, suggesting possible regional differences in cartilage matrix composition between these two groups. Receiver operating characteristic (ROC) analysis showed that subregional analysis in femoral cartilage was more sensitive in discriminating FAI joint cartilage from that of healthy joints than global analysis of the whole region ($T_{1\rho}$: area under the curve (AUC) = 0.981, P = 0.0001 for R9 sub-region; AUC = 0.901, P = 0.002 for whole region; T_2: AUC = 0.976, P = 0.0005 for R9 sub-region; AUC = 0.808, P = 0.0124 for whole region). The results of this study demonstrated regional variations in hip cartilage composition using MR relaxation times ($T_{1\rho}$ and T_2) and suggested that analysis based on local regions was more sensitive than global measures in subjects with and without FAI.

Keywords

MRI; Hip; Cartilage; $T_{1\rho}$ and T_2; Femoral-acetabular impingement

☆Institution at which the study performed: University of California San Francisco.

☆☆Funding Source: NIH/NIAMS P50 AR060752 (SM), NIAMS U01 AR055079 (SM).

*Corresponding author. Tel.: +1 415 514 4025; fax: +1 415 514 4956. subburaj@radiology.ucsf.edu (K. Subburaj).

1. Introduction

Over the past decade, conditions such as femoroacetabular impingement (FAI) [1–4] and acetabular dysplasia [5,6] have been identified as pertinent causes of premature osteoarthritis (OA) of the hip joint in young and middle-aged patients [7]. Cam-type FAI, characterized by an anatomic deformity at the femoral head-neck junction, is known to affect the pathogenesis of hip OA [8,9]. Similarly, a range of normal anatomy at the femoral head-neck junction suggests that not all anatomic variations result in joint degeneration. Surgical treatment has been recommended to reduce clinical symptoms and to delay the onset of OA. The outcome of surgical intervention depends on the degree of pre-existing OA with naturally poorer results in patients with advanced changes. Thus, early detection of cartilage degeneration could help identify patients with hip pain who may benefit from early surgical intervention. The biomechanical stresses in the soft tissues depend strongly on the femoral head and acetabular geometry. Computational and imaging studies have shown that, in impinging joints, day-to-day activities involving extensive motion, inducing excessive distortion and shearing of the tissue-bone interface and high contact stress [8,9], lead to morphological and structural damage [9].

Structural anatomy and the extent of hip OA are typically assessed by the plain radiography; however, this imaging modality is known to be insensitive to early stages of OA. The need to noninvasively detect the earliest changes in the degeneration of articular cartilage in order to implement and validate potential early therapeutic interventions has stimulated considerable interest in the development of techniques, like quantitative magnetic resonance imaging (MRI) that can directly probe the macromolecular structure. The utilization of MRI to assess in-vivo cartilage morphology (volume and thickness) [10], anatomical alterations (lesions), composition, and functional properties [11] has received considerable interest in recent years. However, evaluation of the articular hip cartilage with MRI is extremely challenging, because of the thinness of the cartilage and spherical surface geometry of the femoral head and acetabulum. Despite significant improvements in MRI technology over the past decade, a major limitation of currently available sequences is their inability to consistently detect superficial degenerative and posttraumatic cartilage lesions that may progress to more advanced OA. $T_{1\rho}$ and T_2 relaxation time mapping have recently emerged as potential markers of early biochemical cartilage degeneration. These measures are highly sensitive to alterations in composition and structural integrity of collagen in the cartilage extracellular matrix in vivo ([12–14]. It is more or less generally agreed in the literature that with increasing degeneration there was an increase in water content and decrease in glycosaminoglycan (GAG) content. It has been shown in literature that the collagen content and its orientation is the major factor in changes of cartilage T_2 relaxation times [13,14]. Mlynarik et al. showed that the relaxation mechanisms ($T_{1\rho}$ and T_2) in articular cartilage are highly dependent on the static magnetic fields [15]. Keenan et al. reported $T_{1\rho}$ relaxation time inversely correlated with glycosaminoglycan (GAG) content in cartilage regions with normal T_2 relaxation time [16]. On the other hand, Menezes et al.[14] and Mlynarik et al. [17], observed focal areas of high and low $T_{1\rho}$ and T_2 which were unexplained by GAG concentration or collagen orientation suggesting macromolecular concentration and/or molecular effects. Though in literature conflicting evidence, regarding contributing factors for the variations in $T_{1\rho}$ and T_2, are reported, it has been agreed that these measures are sensitive to identify alterations in ECM composition and macromolecular structure and integrity. While these MRI techniques have been investigated extensively in the knee, their application to the hip has been relatively limited despite its importance, in part due to signal-to-noise ratio constraints associated with the deeper position of this joint.

Due to the thin, adhesive nature of the two articular hip cartilage layers, morphological and relaxometry analysis of this tissue has generally considered the two layers (femoral and

acetabular) as a single unit [10]. However, the biomechanical loading of the hip joint and thus the degenerative changes in Osteoarthritis (OA) may vary locally, depending on the physical activity being performed, anatomy of the joint, and the composition of the cartilage [18,9], thus emphasizing the need for regional analysis of healthy and degenerated hip cartilage. We tested the hypothesis that an analysis based on local regions of the hip cartilage is more sensitive than global measures of hip cartilage morphometry and composition.

We devised a method to automatically divide the femoral and acetabular cartilage into regional segments using anatomical and image coordinates and demonstrate regional variations in healthy volunteers and subjects with femoral acetabular impingement. We specifically aimed to demonstrate that [1] MR relaxation times ($T_{1\rho}/T_2$) in these sub-regions are significantly different from those of the full region of interest (complete femoral and acetabular cartilage), and that [2] sub-regional analysis of $T_{1\rho}/T_2$ relaxation times better discriminates subjects with FAI from healthy controls.

2. Materials and methods

2.1. Subjects

Twelve healthy volunteers (Age = 29.9 ± 10.9 years, range = 22–60 years; BMI = 23.5 ± 2.8 kg/m^2, range = 17.9–28.1 kg/m^2) and 9 subjects who presented with symptomatic FAI based on clinical examination and plain radiographic findings [19] (Age = 36.6 ± 9.7 years, range = 23–52 years; BMI = 26.2 ± 6.9 kg/m^2, range = 18.8–38.4 kg/m^2) were recruited as a part of a large cohort study approved by the institutional review board of our institution. All subjects signed informed consent and Health Insurance Portability and Accountability Act (HIPAA) forms prior to data collection.

2.2. MR image acquisition

All imaging was performed with a 3-Tesla MR scanner (GE MR750, GE Healthcare, Waukesha, WI) and a cardiac coil (GE Healthcare, Waukesha, WI). Patient positioning aids were used to immobilize and support patients, the coil was positioned reproducibly lateral and anterior to the joint of interest, and there was a consistent, reproducible, and comfortable hip positioning during scanning. Participants were positioned supine, with the knees extended and the feet held together by adhesive tape for standardizing the hip and knee angles. The imaging protocol included sagittal and coronal T_2-weighted fat-saturated fast spin-echo (FSE) images (TR/TE = 3678/60 msec, field of view (FOV) = 14 cm, matrix = 288×224, slice thickness = 4 mm, no gap, echo train length [ETL] = 16, band-width = 50 kHz, NEX = 4, scan time = 3.5 minutes each) for clinical grading, oblique axial T_2-weighted FSE images (slice thickness = 3 mm, no gap, matrix = 288×224, FOV = 18 cm, scan time = 4 minutes) for alpha angle (α) measurement, high resolution, fat-suppressed, sagittal 3D fat-suppressed spoiled gradient echo (SPGR) images (TR/TE = 30.4/12.6 msec, slice thickness = 1.5 mm, in-plane resolution = 0.27 mm, matrix = 512×512, FOV = 14 cm, scan time = 9.20 minutes) for cartilage morphology assessment, and a combined $T_{1\rho}/T_2$ quantification sequence [20], allowing post-processing creation of $T_{1\rho}$ and T_2 maps. The combined sequence is composed of two parts: magnetization preparation for either $T_{1\rho}$ or T_2 weighting, followed by a 3D SPGR acquisition during transient signal evolution immediately after magnetization preparation. A flag is defined in the pulse sequence to switch between $T_{1\rho}$ and T_2 preparation according to numbers of time of spin-lock (TSL) and time of echo (TE) defined (for $T_{1\rho}$ preparation: time of spin lock [TSL] = 0/15/30/45 msec, spin-lock frequency = 500 Hz, views per segment (VPS) = 64, time of recovery = 1.2 sec; for T_2 preparation: TE = 0/10.4/20.8/41.7 msec; for both for $T_{1\rho}$ and T_2: FOV = 14 cm, matrix = 256×128, views per segment (VPS) = 64, bandwidth = 62.5 kHz, time of recovery

= 1.2 sec, slice thickness = 4 mm, no gap, in-plane resolution = 0.5 mm, scan time = 13.40 minutes). The raw data of the MR images were acquired with the matrix 256×128, and then interpolated on the k-space in order to obtain the MR images with the matrix of 256×256. To evaluate reproducibility, all images for a subset of healthy subjects (all males, mean age = 23 ± 3.6 years, N = 4) were acquired twice in the same session, and subjects were repositioned in between scans.

2.3. MR image analysis

All MR images were reviewed by an experienced musculoskeletal radiologist (TML) to evaluate focal cartilage abnormalities, labral tears, bone marrow edema pattern as well as other morphological abnormalities; based on femoral-head deformities with concurrent cartilage and labral abnormalities as well as increased alpha angles [21] and typical clinical findings subjects were categorized into the FAI group. All but one of the FAI patients had cam-type deformity. MR images were transferred to a HP workstation (Hewlett-Packard, Palo Alto, CA) for off-line quantification of MR relaxation times ($T_{1\rho}$ and T_2). Fig. 1 shows the operational flow of data processing. Cartilage regions of interest were defined on sagittal 3D high-resolution SPGR images using an in-house software program based on a spline-based semi-automated (automated Gaussian-Laplacian filtering-based noise reduction and edge detection and manual correction) segmentation algorithm in MATLAB (Mathworks Inc, El Segundo, CA) [22]. Cartilage segmentation was defined into three regions of interest: acetabulum, femur, and the combination of the two (called bi-layered) (Fig. 2). Quality control readings of all segmentations were performed an experienced musculoskeletal radiologist (TML) before quantification. A sphere was fitted to the contours of the bone-cartilage of the femur head and the center of the sphere was taken as the fitted center of the femoral head (C_{FH}) for further computation. Starting from C_{FH}, the sphere was divided was divided into 4 quadrants (anterior-superior, anterior-inferior, posterior-superior, and posterior-inferior sub-regions) by vertical (P_v) and horizontal (P_h) planes, parallel to the coronal and axial imaging planes respectively, passing through C_{FH}. Then each quadrant (e.g. anterior-superior) was further divided into three equal sub-regions (30° intervals), for a total of 12 regions, thereof only 9 sub-regions (R2–R10) contained cartilage. For acetabular cartilage analysis, only sub-regions R2 to R8 contained cartilage.

The $T_{1\rho}$ and T_2 maps were reconstructed by fitting the image intensity (voxel-by-voxel) to the equation below using a Levenberg-Marquardt mono-exponential fitting algorithm developed in-house: $S_{TSL} = S_0\, e^{-TSL/T1\rho}$ for $T_{1\rho}$ fitting, where S_0 is the signal intensity when TSL = 0 ms; $S_{TE} = S_0\, e^{-TE/T2}$ for T_2 fitting, where S_0 is signal intensity when preparation TE = 0. To minimize the error due to motion between the scans, $T_{1\rho}$- and T_2-weighted images with the shortest TSL = 0 and TE = 0 (therefore with highest SNR) were rigidly registered to high-resolution SPGR images acquired in the same examination using the VTK CISG Registration Toolkit (Kitware Inc., Clifton Park, NY). The transformation matrix was applied to the reconstructed $T_{1\rho}$ and T_2 maps. The original splines of segmented cartilage contours from the high-resolution SPGR images were superimposed on the corresponding reconstructed $T_{1\rho}$ and T_2 maps to define the regions of interest (ROIs) for $T_{1\rho}$ and T_2 assessment. To reduce artifacts caused by partial volume effects with synovial fluid, regions were corrected to exclude fluid pixels on the relaxation-time map before quantification.

2.4. Statistical analysis

Reproducibility $T_{1\rho}$ and T_2 measurements were determined by calculating the coefficients of variation (CV_{RMS}). To assess the differences in $T_{1\rho}$ and T_2 in the sub-divided regions compared to that of the global region, a student's t-test was performed. Analysis of variance (ANOVA) was used to identify whether the differences in mean MR relaxation times

between control group and FAI group differed between the sub-regions of the cartilage. Post hoc tests were then used to identify which sub-regions demonstrated significant differences between groups. The ability of mean values of global ROIs and different sub-regions of the cartilage to discriminate between healthy controls and subjects with FAI was assessed using the area under the curve (AUC) of the receiver operating characteristic (ROC) curve analysis. The significance of the discriminations was evaluated with a two-tailed t-test. All statistical analysis was performed using JMP 7.0 (SAS Institute, Cary, NC). The significance level was set to 5% and p-values were adjusted for the 9 sub-regions, considered for analysis, based on the Bonferroni method.

3. Results

3.1. Reproducibility

Coefficient of variation values for measuring reproducibility of relaxation time measurement ranged from 1.2% to 3.3% for $T_{1\rho}$ and 3.1% to 4.7% for T_2. The reproducibility of $T_{1\rho}$ and T_2 measurements in subregions of the cartilage was as follows: for $T_{1\rho}$ (range = 1.2–2.8%), R3 = 2.1%; R4 = 2.8%; R5 = 2.4%; R6 = 1.8%; R7 = 1.6%; R8 = 1.2%; R9 = 1.4%; R10 = 1.9% and for T_2 (range = 1.5–3.1%), R3 = 2.4%; R4 = 2.6%; R5 = 3.1%; R6 = 1.9%; R7 = 1.7%; R8 = 1.5%; R9 = 1.8%; R10 = 2.1%.

3.2. Global $T_{1\rho}$ and T_2 measurements

Representative Color-coded $T_{1\rho}$ and T_2 maps overlaid on first-echo MR images are shown in Fig. 3. The mapping of the cartilage $T_{1\rho}$ and T_2 maps onto the 3-D representation of the segmented femoral head are shown in Fig. 4. The $T_{1\rho}$ and T_2 times in the bi-layered (i.e. combined femoral and acetabular cartilage), femoral, and acetabular cartilage regions of interest of the controls and FAI subjects are given in Table 1.

3.3. Sub-regional analysis of $T_{1\rho}$ and T_2 measurements

With respect to the first objective, this analysis determined whether MR relaxation times ($T_{1\rho}$ and T_2) in sub-regions (Fig. 3) are significantly different from the whole ROI in healthy subjects. The detailed results of $T_{1\rho}$ and T_2 measurements in these sub-regions and whole ROIs are shown in Fig. 5. The $T_{1\rho}$ relaxation times of sub-regions R9 (30.4 ± 2.5 msec, P = 0.0025) and R10 (30.5 ± 2.1 msec, P = 0.0002) in femoral cartilage were significantly lower than that of the whole cartilage ROI (35.5 ± 2.4 ms). In the acetabular layer, R7 (30.7 ± 3.7 msec, P = 0.0020) and R8 (23.9 ± 3.3 msec, P = <0.0001) had significantly lower $T_{1\rho}$ values than the whole ROI (35.4 ± 2.8 msec). When we investigated T_2 relaxation times separately and compared them with those in the bi-layered cartilage ROIs, only subregion R9 (26.5 ± 2.7 msec, P = 0.0003) was significantly different from the whole ROI (31.1 ± 1.9 ms). In the femoral cartilage layer, sub-regions R9 (26.3 ± 2.7 msec, P = 0.004) and R10 (27.2 ± 3.0 msec, P = 0.0003) had significantly lower T_2 times than the whole ROI (31.0 ± 1.7 msec). In the acetabular layer, sub-region R8 (21.2 ± 4.7 msec, P = <0.0001) had a significantly lower mean T_2 value than the whole ROI (31.0 ± 2.3 msec).

The second objective of this study was to demonstrate that the sub-regional analysis better differentiates subjects with FAI from the healthy controls. When we analyzed the sub-regional $T_{1\rho}$ relaxation times using ROC analysis (Fig. 6), the sub-region R9 better accomplished this task than the whole ROI in both bi-layered (AUC = 0.981, P = 0.0001 for R9 sub-region; AUC = 0.835, P = 0.0127 for whole region) and femoral cartilage (AUC = 0.981, P = 0.0001 for R9; AUC = 0.901, P = 0.002 for whole region). Also, higher AUC values were observed in anterior-superior sub-regions R7 and R8 of all (bi-layered, femoral and acetabular) cartilages (Table 2). Sub-regional analysis of T_2 relaxation times showed that the R9 sub-region better discriminated both the groups than the whole region of interest

in both the bi-layered ROIs (AUC = 0.953, P = 0.0026 for R9 subregion; AUC = 0.795, P = 0.0417 for whole region) as well as in femoral cartilage (AUC = 0.976, P = 0.0005 for R9 sub-region; AUC = 0.808, P = 0.0124 for whole region).

Our results also showed that sub-region R9 in both the bi-layered and femoral cartilage ROIs showed significantly different MR relaxation times ($T_{1\rho}$ and T_2) between FAI and controls ($T_{1\rho}$: 39.0 ± 4.3 msec vs. 30.4 ± 2.5 msec, P = 0.0002; T_2: 32.6 ± 2.9 msec vs. 26.5 ± 2.7 msec, P = 0.0035).

4. Discussion

In this study, we developed an automatic method for sub-regional analysis of variations in MR relaxation times of hip cartilage, and demonstrated that analysis based on local regions was more sensitive than global measures of the same parameters in hip cartilage for discriminating subjects with and without FAI. Our results showed that (a) $T_{1\rho}$ and T_2 relaxation times in the anterior-superior cartilage sub-region were significantly different from those of the global cartilage ROI, and (b) the anterior-superior cartilage region was more sensitive in discriminating subjects with FAI from those without than the global regions of interest.

The reported $T_{1\rho}$ (31.8–41.4 msec) and T_2 (28.4–33.6 msec) values in this study are in the expected range compared with previously reported $T_{1\rho}$ (33.79–45.47 msec) [10] and T_2 (29.4–33.4 msec) [10,23,24] relaxation times of normal hip joint cartilage. Short-term reproducibility indicates that in-vivo hip cartilage $T_{1\rho}$ and T_2 measurements are highly reproducible (CV < 5%).

Longer cartilage relaxation times ($T_{1\rho}$ and T_2) were observed in subjects with FAI than healthy controls. Similarly, Carballido-Gamio et al. [10] reported longer a $T_{1\rho}$ and T_2 relaxation times in a subject with mild hip OA compared to controls. Nishii et al. [24] also observed longer T_2 values in a group with early OA compared to a control group of volunteers, though his group analyzed only mid-coronal slices of the hip cartilage in subjects with hip dysplasia. Several studies have reported that, T_2 is sensitive to changes in hydration, collagen concentration [25], and orientation of the highly organized anisotropic arrangement of collagen fibrils in the extracellular cartilage matrix [13,26]. It has been observed that with progression of knee OA, morphological parameters such as cartilage thickness and volume decrease [27], and that molecular and biochemical cartilage properties such as T_2 relaxation time [13], $T_{1\rho}$ relaxation time [28] increase. T_2 measurement is widely used to assess the macromolecular constitution of cartilage, but collagen concentration and orientation alters the relaxation rate. On the other hand, changes in collagen orientation may be among the first changes to occur and can be visualized by T_2 mapping. Cardenas-Blanco et al. also observed elevated $T_{1\rho}$ relaxation times in symptomatic FAI subjects than in controls [29]. Regatte et al., found that $T_{1\rho}$-weighted MR imaging is more sensitive to proteoglycan depletion than T_2-weighted MR imaging [30,31]. The primary mechanisms that contribute to cartilage $T_{1\rho}$ are from dipolar relaxation and chemical exchange, which are affected by the changes in macromolecular content and structure. Studies have shown that the $T_{1\rho}$ dispersion is primarily due to residual dipolar interaction and contribution due to chemical exchange between –OH and –NH groups of proteoglycan (PG) with bulk water is only ~6% at 3 T [12,15,32]. Keenan et al. observed higher $T_{1\rho}$ relaxation time in cartilage regions with lower GAG content [16]. On the other hand, Menezes et al. reported that collagen concentration may be the dominant factor in determining $T_{1\rho}$ and T_2 relaxation, but cautioned against concluding observed differences in $T_{1\rho}$ and T_2 to concentration differences or orientation differences [14]. They have observed focal regions of high and low $T_{1\rho}$ and T_2 which were unexplained by GAG concentration or collagen orientation

suggesting macromolecular concentration and/or molecular effects. Similar results were reported by Mlynarik et al. [17] also. We also observed a larger dynamic range for $T_{1\rho}$ compared to T_2 in both subjects with FAI and healthy controls, which agrees with earlier studies on subjects with knee OA [10], FAI [29], and healthy controls [24,27]. The understanding of the behavior of these biomarkers derived from MRI in characterizing hip cartilage and degeneration is still in the early stages. This study demonstrates that $T_{1\rho}$ and T_2 may be a valuable biomarker in identifying subjects with pathological risks to progression to OA, and could allow one to quantifying and potentially monitor structural and biochemical changes that occur in early degeneration.

Significantly different $T_{1\rho}$ and T_2 relaxation times in the anterior-superior regions (R7, R8, and R9) of the hip joint cartilage suggest possible regional differences in cartilage matrix composition between subjects with FAI and healthy subjects. ROC analysis showed that subregional analysis especially in anterior-superior regions in femoral and acetabular cartilage better discriminate FAI joints from the healthy joints. It has been recognized that FAI can cause premature OA if appropriate intervention is not performed early [3]. Bittersohl et al. [33] observed that in subjects with cam-type FAI, focal cartilage damage was most frequent in the superior-anterior regions (similar to R7, R8 and R9 sub-regions in this study) and the damage pattern was well localized (reflected by the T_1 value distribution). Cardenas-Blanco et al. also observed significantly elevated $T_{1\rho}$ relaxation times in anterior (R9 and R8 sub-regions in this study) and anterior-superior regions (R7 and R8 sub-regions in this study) of the hip cartilage in symptomatic FAI subjects than in controls [29]. The collagen fibers have an ordered structure, making the water associated with them exhibit both magnetization transfer and magic angle (collagen fibers orientation to the applied static magnetic field B_0) effects [13,34]. Because of its curved surface, the hip joint cartilage is susceptible to magic angle effect. Cova et al. observed regional differences in signal intensity of hip cartilage and suggested this behavior may be due to the anisotropic arrangement of collagen fibers within a specific zone [35]. These regions overestimate the mean $T_{1\rho}$ and T_2 relaxation times, which makes the relaxation times in anterior and anterior-superior sub-regions (R9 and R10) with perpendicular orientation of collagen fibers relative to the B_0 field significantly lower than the global mean. But the influence of regional difference in composition, biological activity, and joint biomechanics on $T_{1\rho}$ and T_2 relaxation times must be taken into consideration while studying the magic angle effect. Stelzeneder et al. [9] also reported that cartilage defects in FAI hips might be of a true focal nature and may not affect the surrounding cartilage, based on relative dGEMRIC indices. Ilizaliturri et al. [36] and Sampson [37] proposed the use of regional zones for precise description of a lesion's position and found that most cartilage lesions from direct damage due to morphologic conflicts resulting from FAI are in zones 2 and 3 (superior and anterior-superior regions) near the fovea (similar to R6–R9 sub-regions in this study). This clearly suggests that the damage due to FAI pathologic deformities appears to be region-specific and the surrounding cartilage regions are less affected (showing less or no change in biochemical composition). In contrast, Kim et al. [38] showed that subjects with hip dysplasia have a more generalized pattern of cartilage damage. Literature suggests that cartilage loss in OA and physiological loading may not be uniform throughout the cartilage plates [23], but may affect certain regions more frequently and more strongly than others, and may thus exhibit a different biochemical composition and degeneration [9,39]. In our cases with cam-type FAI, significantly elevated $T_{1\rho}$ and T_2 relaxation times were observed in the anterior to superior regions of the cartilage that reflects the change in biochemical composition in those regions. These findings are consistent with previous studies in literature on location of hip joint cartilage lesions in FAI patients [29,33,37]. The damage in those regions may be caused from impaction of the head, demarcation zones from FAI, and subchondral cysts secondary to FAI. In this study, we successfully developed a method for measuring regional variations in cartilage composition in anatomically different sub-regions

of articular hip cartilage. We also demonstrated that sub-regional analysis was more sensitive in discriminating subjects with FAI from healthy controls.

ROC analysis showed that sub-regions in femoral cartilage better discriminated FAI joints from the healthy ones. Though the AUC values in ROC analysis were similar in both ROIs (femoral cartilage and bi-layered cartilage), femoral cartilage sub-regions ROI showed better performance in differentiating the two groups. Acetabular cartilage sub-regions on the other hand show significance in only $T_{1\rho}$ values in differentiating the two groups. These results suggest that analyzing hip cartilage as a single ROI (i.e. a bi-layered cartilage unit) may not be as efficacious as examining separate femoral and acetabular cartilaginous ROIs in the classification of subjects with hip abnormalities. The global mean $T_{1\rho}$ and T_2 values in bi-layered and acetabular cartilage regions were not significantly different between subjects with and without FAI, as they were in the femoral cartilage. This suggests that the analysis of individualized (femoral and acetabular) regions of interest gives better insight on region-specific degeneration and allow us to exclude joint fluid with high signal intensity between the acetabular and femoral cartilage layers during quantification [23,33].

The limitations of our study have to be considered while interpreting the findings. The number of subjects was small (12 healthy subjects and 9 FAI patients). Cartilage $T_{1\rho}$ and T_2 relaxation times were assessed only in central regions of sagittal hip joint images, and medial and lateral areas were not evaluated because the curved joint surface that is susceptible to partial volume effect [10]. Although the magic angle effect has been discussed in the literature for T_2 [34,40] and $T_{1\rho}$ [32,34,41] in knee cartilage or cartilage specimens, no studies, to our knowledge, have documented an orientation dependence of T_2 and $T_{1\rho}$ in cartilage of the hip joint in vivo [35] and its effect on measures within sub-regions, which needs to be further investigated. Furthermore, delineation of the cartilage surface and defining regions of interest for quantification of femur and acetabulum separately was difficult and may be improved using a device to induce continuous leg traction during the image acquisition [24] or better pulse sequences that provide brighter signal intensity from fluid than the conventional sequences, such as multi-echo recombined gradient echo sequence [42]. The latter would also reduce the partial volume artifact on the superficial layer (voxels closer to the articular surface) of the cartilage, which would be useful for laminar analysis of MR relaxation times [18,24].

In summary, this study demonstrated (a) regional analysis of cartilage relaxation times ($T_{1\rho}$ and T_2) in the hip joint is highly reproducible, (b) variations in regional composition at the hip cartilage using MR relaxation times ($T_{1\rho}$ and T_2), and (c) that analysis based on local regions is more sensitive than global measures of hip cartilage composition and that cartilage degeneration in subjects with and without femoral-acetabular impingement may be region-specific.

References

1. Clohisy JC, Beaule PE, O'Malley A, Safran MR, Schoenecker P. AOA symposium. Hip disease in the young adult: current concepts of etiology and surgical treatment. J Bone Joint Surg Am. 2008; 90(10):2267–81. [PubMed: 18829926]
2. Leunig M, Beaule PE, Ganz R. The concept of femoroacetabular impingement: current status and future perspectives. Clin Orthop Relat Res. 2009; 467(3):616–22. [PubMed: 19082681]
3. Beck M, Kalhor M, Leunig M, Ganz R. Hip morphology influences the pattern of damage to the acetabular cartilage: femoroacetabular impingement as a cause of early osteoarthritis of the hip. J Bone Joint Surg Br. 2005; 87(7):1012–8. [PubMed: 15972923]
4. Ganz R, Parvizi J, Beck M, Leunig M, Notzli H, Siebenrock KA. Femoroacetabular impingement: a cause for osteoarthritis of the hip. Clin Orthop Relat Res. 2003; 417:112–20. [PubMed: 14646708]

5. Jacobsen S. Adult hip dysplasia and osteoarthritis. Studies in radiology and clinical epidemiology. Acta Orthop Suppl. 2006; 77(324):1–37. [PubMed: 17380595]
6. Lievense AM, Bierma-Zeinstra SM, Verhagen AP, Verhaar JA, Koes BW. Influence of hip dysplasia on the development of osteoarthritis of the hip. Ann Rheum Dis. 2004; 63(6):621–6. [PubMed: 15140766]
7. Anderson LA, Peters CL, Park BB, Stoddard GJ, Erickson JA, Crim JR. Acetabular cartilage delamination in femoroacetabular impingement. Risk factors and magnetic resonance imaging diagnosis. J Bone Joint Surg Am. 2009; 91(2):305–13. [PubMed: 19181974]
8. Chegini S, Beck M, Ferguson SJ. The effects of impingement and dysplasia on stress distributions in the hip joint during sitting and walking: a finite element analysis. J Orthop Res. 2009; 27(2):195–201. [PubMed: 18752280]
9. Stelzeneder D, Mamisch TC, Kress I, Domayer SE, Werlen S, Bixby SD, et al. Patterns of joint damage seen on MRI in early hip osteoarthritis due to structural hip deformities. Osteoarthritis Cartilage. 2012; 20(7):661–9. [PubMed: 22469848]
10. Carballido-Gamio J, Link TM, Li X, Han ET, Krug R, Ries MD, et al. Feasibility and reproducibility of relaxometry, morphometric, and geometrical measurements of the hip joint with magnetic resonance imaging at 3 T. J Magn Reson Imaging. 2008; 28(1):227–35. [PubMed: 18581346]
11. Subburaj K, Souza RB, Stehling C, Wyman BT, Le Graverand-Gastineau MP, Link TM, et al. Association of MR relaxation and cartilage deformation in knee osteoarthritis. J Orthop Res. 2012; 30(6):919–26. [PubMed: 22161783]
12. Duvvuri U, Goldberg AD, Kranz JK, Hoang L, Reddy R, Wehrli FW, et al. Water magnetic relaxation dispersion in biological systems: the contribution of proton exchange and implications for the noninvasive detection of cartilage degradation. Proc Natl Acad Sci U S A. 2001; 98(22): 12479–84. [PubMed: 11606754]
13. Mosher TJ, Dardzinski BJ. Cartilage MRI T2 relaxation time mapping: overview and applications. Semin Musculoskelet Radiol. 2004; 8(4):355–68. [PubMed: 15643574]
14. Menezes NM, Gray ML, Hartke JR, Burstein D. T2 and T1rho MRI in articular cartilage systems. Magn Reson Med. 2004; 51(3):503–9. [PubMed: 15004791]
15. Mlynarik V, Szomolanyi P, Toffanin R, Vittur F, Trattnig S. Transverse relaxation mechanisms in articular cartilage. J Magn Reson. 2004; 169(2):300–7. [PubMed: 15261626]
16. Keenan KE, Besier TF, Pauly JM, Han E, Rosenberg J, Smith RL, et al. Prediction of glycosaminoglycan content in human cartilage by age, T1rho and T2 MRI. Osteoarthritis Cartilage. 2011; 19(2):171–9. [PubMed: 21112409]
17. Mlynarik V, Trattnig S, Huber M, Zembsch A, Imhof H. The role of relaxation times in monitoring proteoglycan depletion in articular cartilage. J Magn Reson Imaging. 1999; 10(4):497–502. [PubMed: 10508315]
18. Watanabe A, Boesch C, Siebenrock K, Obata T, Anderson SE. T2 mapping of hip articular cartilage in healthy volunteers at 3 T: a study of topographic variation. J Magn Reson Imaging. 2007; 26(1):165–71. [PubMed: 17659572]
19. Tannast M, Siebenrock KA, Anderson SE. Femoroacetabular impingement: radiographic diagnosis – what the radiologist should know. AJR Am J Roentgenol. 2007; 188(6):1540–52. [PubMed: 17515374]
20. Li JSX, Liang F, Vishnudas KS, Chen W, Banerjee S, Majumdar S. Simultaneous acquisition of T1rho and T2 quantification in cartilage – reproducibility and diurnal variation. Proc Intl Soc Mag Reson Med. 2011:19.
21. Pfirrmann CW, Mengiardi B, Dora C, Kalberer F, Zanetti M, Hodler J. Cam and pincer femoroacetabular impingement: characteristic MR arthrographic findings in 50 patients. Radiology. 2006; 240(3):778–85. [PubMed: 16857978]
22. Carballido-Gamio J, Bauer J, Lee KY, Krause S, Majumdar S. Combined image processing techniques for characterization of MRI cartilage of the knee. Conf Proc IEEE Eng Med Biol Soc. 2005; 3:3043–6. [PubMed: 17282885]
23. Nishii T, Shiomi T, Tanaka H, Yamazaki Y, Murase K, Sugano N. Loaded cartilage T2 mapping in patients with hip dysplasia. Radiology. 2010; 256(3):955–65. [PubMed: 20720077]

24. Nishii T, Tanaka H, Sugano N, Sakai T, Hananouchi T, Yoshikawa H. Evaluation of cartilage matrix disorders by T2 relaxation time in patients with hip dysplasia. Osteoarthritis Cartilage. 2008; 16(2):227–33. [PubMed: 17644363]
25. Liess C, Lusse S, Karger N, Heller M, Gluer CC. Detection of changes in cartilage water content using MRI T2-mapping in vivo. Osteoarthritis Cartilage. 2002; 10(12):907–13. [PubMed: 12464550]
26. Burstein D, Gray M, Mosher T, Dardzinski B. Measures of molecular composition and structure in osteoarthritis. Radiol Clin North Am. 2009; 47(4):675–86. [PubMed: 19631075]
27. Li X, Benjamin Ma C, Link TM, Castillo DD, Blumenkrantz G, Lozano J, et al. In vivo T(1rho) and T(2) mapping of articular cartilage in osteoarthritis of the knee using 3 T MRI. Osteoarthritis Cartilage. 2007; 15(7):789–97. [PubMed: 17307365]
28. Li X, Pai A, Blumenkrantz G, Carballido-Gamio J, Link T, Ma B, et al. Spatial distribution and relationship of T1rho and T2 relaxation times in knee cartilage with osteoarthritis. Magn Reson Med. 2009; 61(6):1310–8. [PubMed: 19319904]
29. Arturo Cardenas-Blanco KR, Andrew Speirs, Ian Cameron, Mark Schweitzer, Paul Beaule. Noncontrast cartilage assessment ($T1_{\rho}$) of the hip in femoroacetabular impingment: Can we predict early changes? Proc Intl Soc Mag Reson Med. 2012; 20:3307.
30. Regatte RR, Akella SV, Borthakur A, Kneeland JB, Reddy R. Proteoglycan depletion-induced changes in transverse relaxation maps of cartilage: comparison of T2 and T1rho. Acad Radiol. 2002; 9(12):1388–94. [PubMed: 12553350]
31. Regatte RR, Akella SV, Lonner JH, Kneeland JB, Reddy R. T1rho relaxation mapping in human osteoarthritis (OA) cartilage: comparison of T1rho with T2. J Magn Reson Imaging. 2006; 23(4): 547–53. [PubMed: 16523468]
32. Akella SV, Regatte RR, Wheaton AJ, Borthakur A, Reddy R. Reduction of residual dipolar interaction in cartilage by spin-lock technique. Magn Reson Med. 2004; 52(5):1103–9. [PubMed: 15508163]
33. Bittersohl B, Steppacher S, Haamberg T, Kim YJ, Werlen S, Beck M, et al. Cartilage damage in femoroacetabular impingement (FAI): preliminary results on comparison of standard diagnostic vs delayed gadolinium-enhanced magnetic resonance imaging of cartilage (dGEMRIC). Osteoarthritis Cartilage. 2009; 17(10):1297–306. [PubMed: 19446663]
34. Mosher TJ, Smith H, Dardzinski BJ, Schmithorst VJ, Smith MB. MR imaging and T2 mapping of femoral cartilage: in vivo determination of the magic angle effect. AJR Am J Roentgenol. 2001; 177(3):665–9. [PubMed: 11517068]
35. Cova M, Toffanin R, Frezza F, Pozzi-Mucelli M, Mlynarik V, Pozzi-Mucelli RS, et al. Magnetic resonance imaging of articular cartilage: ex vivo study on normal cartilage correlated with magnetic resonance microscopy. Eur Radiol. 1998; 8(7):1130–6. [PubMed: 9724424]
36. Ilizaliturri VM Jr, Byrd JW, Sampson TG, Guanche CA, Philippon MJ, Kelly BT, et al. A geographic zone method to describe intra-articular pathology in hip arthroscopy: cadaveric study and preliminary report. Arthroscopy. 2008; 24(5):534–9. [PubMed: 18442685]
37. Sampson TG. Arthroscopic treatment for chondral lesions of the hip. Clin Sports Med. 2011; 30(2):331–48. [PubMed: 21419959]
38. Kim YJ, Jaramillo D, Millis MB, Gray ML, Burstein D. Assessment of early osteoarthritis in hip dysplasia with delayed gadolinium-enhanced magnetic resonance imaging of cartilage. J Bone Joint Surg Am. 2003; 85-A(10):1987–92. [PubMed: 14563809]
39. Wirth W, Eckstein F. A technique for regional analysis of femorotibial cartilage thickness based on quantitative magnetic resonance imaging. IEEE Trans Med Imaging. 2008; 27(6):737–44. [PubMed: 18541481]
40. Xia Y, Zheng S. Reversed laminar appearance of articular cartilage by T1-weighting in 3D fat-suppressed spoiled gradient recalled echo (SPGR) imaging. J Magn Reson Imaging. 2010; 32(3): 733–7. [PubMed: 20815075]
41. Li X, Cheng J, Lin K, Saadat E, Bolbos RI, Jobke B, et al. Quantitative MRI using T1rho and T2 in human osteoarthritic cartilage specimens: correlation with biochemical measurements and histology. Magn Reson Imaging. 2011; 29(3):324–34. [PubMed: 21130590]

42. White ML, Zhang Y, Healey K. Cervical spinal cord multiple sclerosis: evaluation with 2D multi-echo recombined gradient echo MR imaging. J Spinal Cord Med. 2011; 34(1):93–8. [PubMed: 21528632]

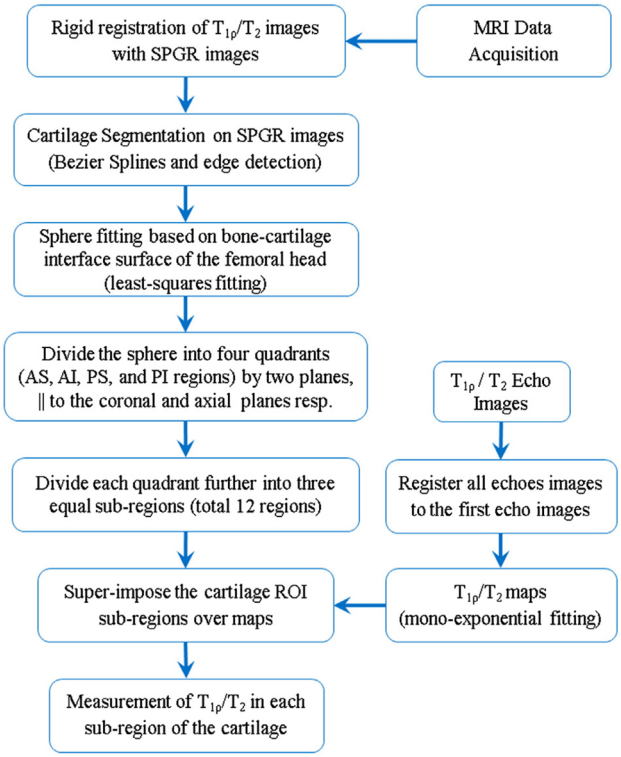

Fig. 1.
Data-flow-diagram of the methodology.

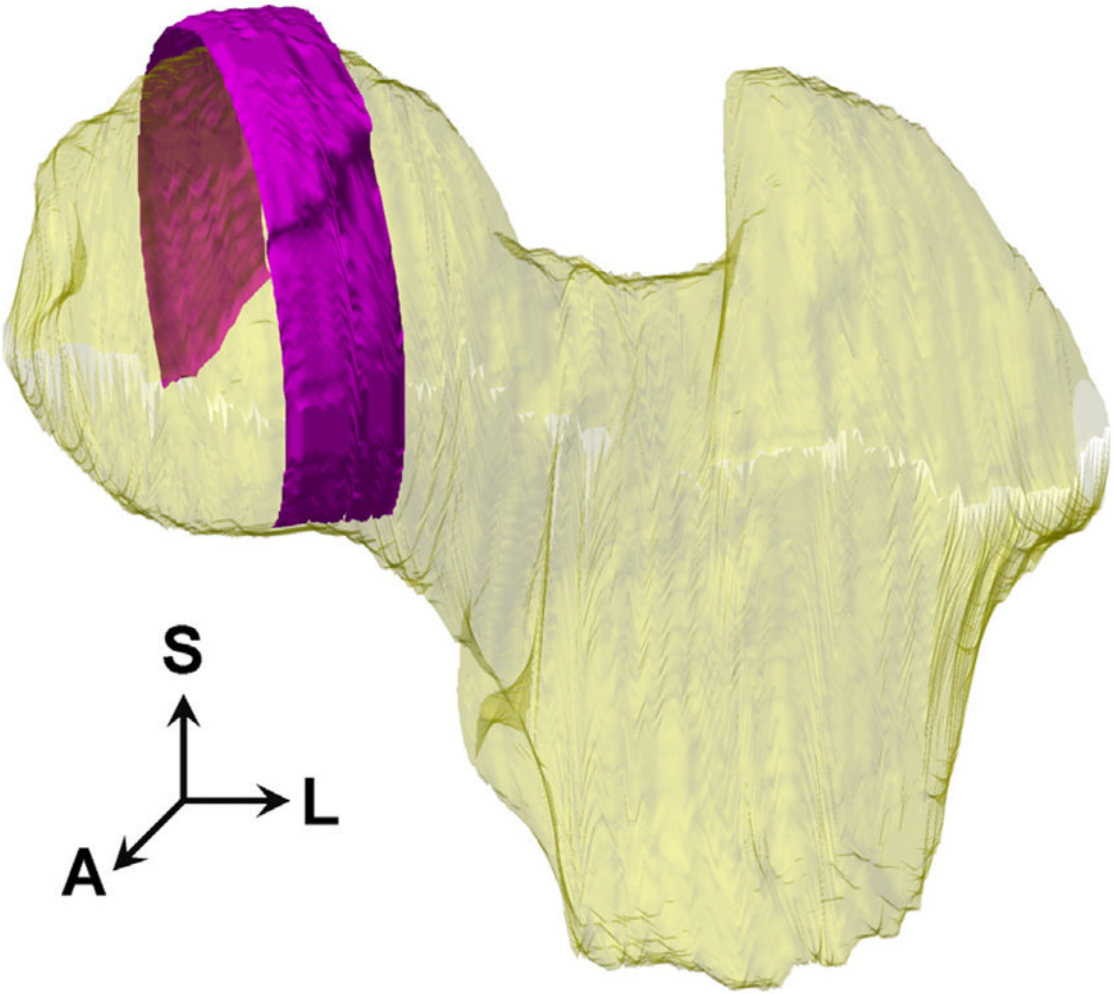

Fig. 2.
3D model of the segmented cartilage superimposed on the femur. A sphere approximating the femoral head was computed from the bone-cartilage interface contours.

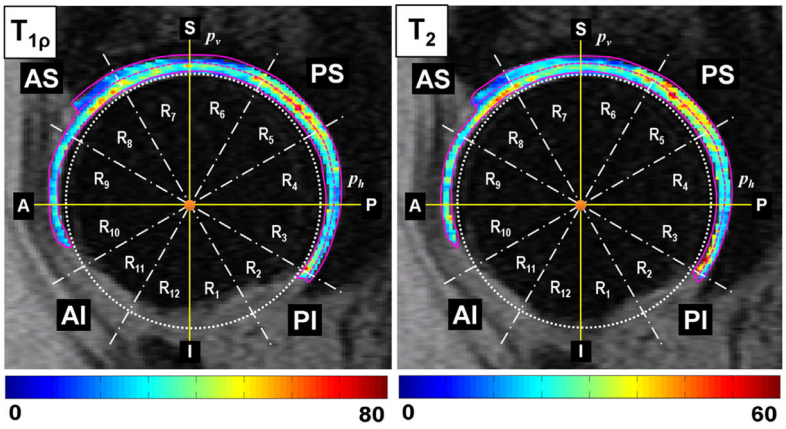

Fig. 3.

Color-coded $T_{1\rho}$ and T_2 relaxation time maps of hip cartilage overlaid on the first echo MR images. Sub-regions for hip joint cartilage assessment (A – Anterior; P – Posterior; S – Superior; I – Inferior; A_S – Anterior-Superior; P_S – Posterior-Superior; A_I – Anterior-Inferior; P_I – Posterior-Inferior; P_h – Horizontal plane; Pv – Vertical plane.) The bar represents the color specific $T_{1\rho}$ and T_2 values in msec.

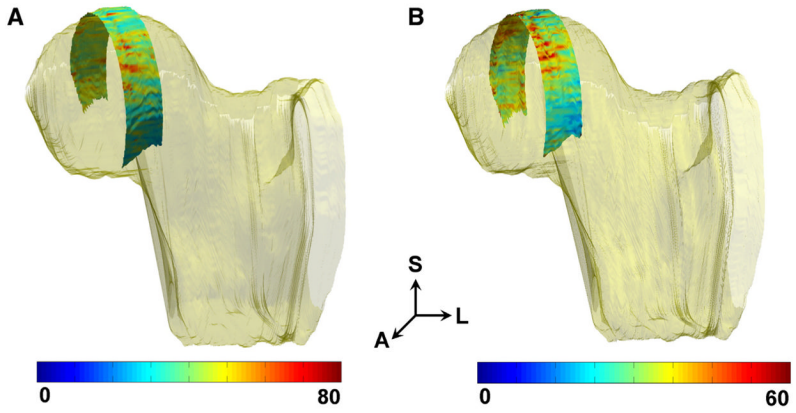

Fig. 4.

Representative three-dimensional $T_{1\rho}$ and T_2 maps of femoral cartilage overlaid on the femoral head. The color bar represents the color specific $T_{1\rho}$ and T_2 values in msec.

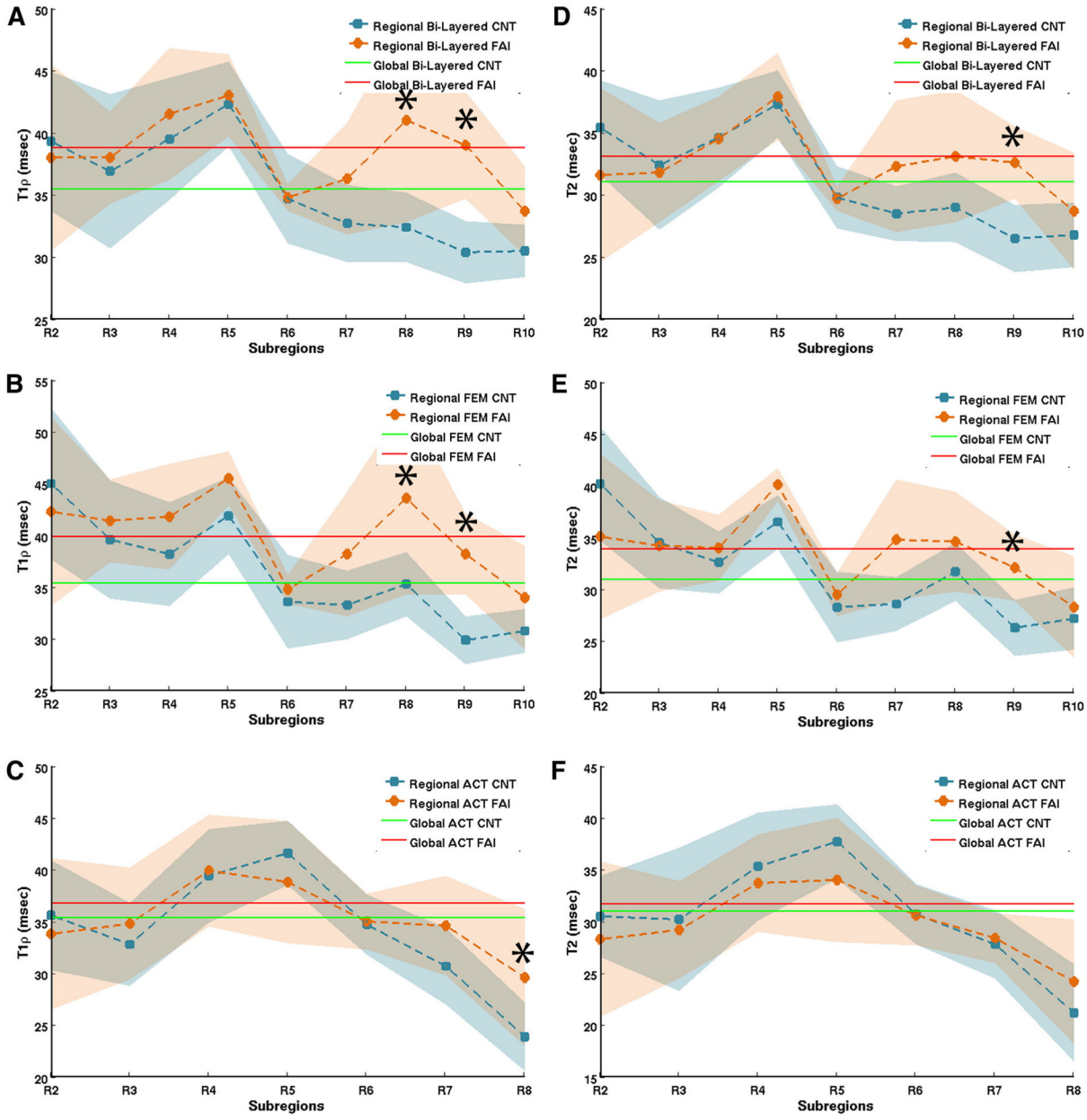

Fig. 5.

Relaxation times in sub-regions of the hip cartilage of controls and FAI patients (A–C) $T_{1\rho}$ relaxation times in bi-layered, femoral and acetabular cartilage regions, (D–F) T_2 relaxation times in bi-layered, femoral and acetabular cartilage regions. Error bars represent standard deviation; (*) represents significant difference between controls and FAI subjects relaxation times.

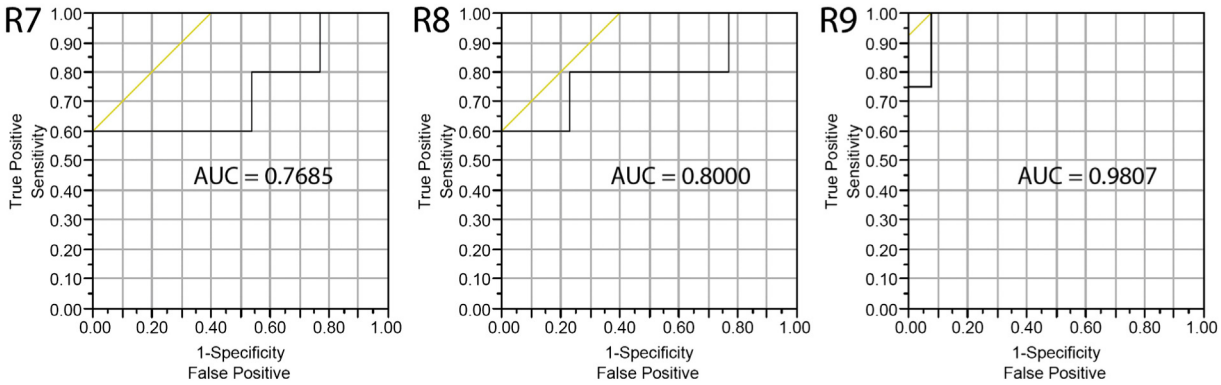

Fig. 6.

Representative ROC curve plots of $T_{1\rho}$ relaxation times in R7, R8, and R9 sub-regions of the femoral cartilage.

Table 1

Global $T_{1\rho}$ and T_2 relaxation time measurements (in msec, mean ± SD) in healthy controls and FAI subjects.

Regions of Interest	$T_{1\rho}$ (msec)			T_2 (msec)		
	Controls	FAI	P-Value	Controls	FAI	P-Value
Bi-Layered Cartilage	35.5 ± 2.4	38.8 ± 2.8	0.0133	31.1 ± 1.9	33.1 ± 1.7	0.0511
Femoral Cartilage	35.4 ± 2.3	39.9 ± 3.3	0.0020	31.1 ± 1.7	33.9 ± 3.1	0.0160
Acetabular Cartilage	35.4 ± 2.8	36.8 ± 3.0	0.3188	31.0 ± 2.3	31.7 ± 2.5	0.5622

Table 2

AUCs of the ROC analysis of mean $T_{1\rho}$ and T_2 values to discriminate between subjects with and without FAI (boldface indicates AUC> = 0.75).

ROI	Acetabular Cartilage		Bi-Layered Cartilage		Femoral Cartilage	
	$T_{1\rho}$	T_2	$T_{1\rho}$	T_2	$T_{1\rho}$	T_2
Whole	0.692	0.6025	0.8352†	0.7948†	0.9011†	0.8076†
R2	0.5083	0.6153	0.4546	0.6346	0.600	0.6923
R3	0.633	0.4821	0.60	0.4821	0.5846	0.4732
R4	0.5167	0.5714	0.6154	0.5000	0.7231	0.6428
R5	0.6833	0.6785	0.6154	0.5536	0.6885	0.6901
R6	0.4179	0.5000	0.4615	0.5892	0.5231	0.5714
R7	0.7709†	0.5952	0.7684†	0.7857†	0.7685†	0.8392†
R8	0.7508†	0.6947	0.7538†	0.7642†	0.8000†	0.7904†
R9			0.9808‡	0.9523†	0.9808‡	0.9761‡
R10			0.7185	0.5476	0.7185	0.5476

†Significant ($p<0.05$) subject discrimination based on ROC analysis.

‡Significant ($p<0.001$) subject discrimination based on ROC analysis.